Journal of Computational Methods in Molecular Design, 2014, 4 (4):68-78

Scholars Research Library
(http://scholarsresearchlibrary.com/archive.html)

ISSN : 2231- 3176
CODEN (USA): JCMMDA

Theoretical study of N-H···O and O-H···N intramolecular hydrogen bonds in the derivatives of 4-(aminomethylene)-1-methylpyrazolin-5-one and its imine tautomer

Zaki S. Safi

Chemistry Department, Faculty of Science, Al Azhar University-Gaza, Gaza, P.O. Box 1277, Palestine

---

ABSTRACT

Intramolecular hydrogen bondings (IHB) in some derivatives of 4-(aminomethylene)-1-methylpyrazolin-5-ones (AMP) and its imine tautomers were investigated using density functional theory (DFT) calculations at B3LYP/6-311+G(d,p) level of theory. The relative stability calculations showed that AMP forms are more stable than IMP ones. The strength of the IHB were investigated by means of several quantum descriptors such as geometrical structural (bond lengths and angles), topological parameters based of Atoms in Molecules theory (AIM) of Bader (total electronic density and its Laplacian at bond critical point (BCP) and ring critical point (RCP)), hyper conjugative interaction energy (E_{CT}), related to the LP(O)→$\sigma^*_{(N–H)}$ and LP(N)→$\sigma^*_{(O–H)}$ overlaps, chemical shifts of the bridged hydrogen atom, δ^1H, frequency shifts of the N-H and O-H stretching vibration modes. The combined results strongly illustrate that the O-H···N exist for IMP forms is stronger that the N-H···O in AMP tautomers. Good linear correlation coefficients between IHB energy, E_{HB}, based on Espinosa's equation and the abovementioned descriptors were reported.

Keywords: 4-(aminomethyle)-1-methylpyrazolin-5-one, Intramolecular hydrogen bond, Density functional theory, Bader's QTAIM**,** IR and NMR.

INTRODUCTION

The tautomerism of organic compounds is one of the most important processes in chemistry. This process often involves intramolecular proton transfer (IPT) between the tautomeric groups, particularly in the gas phase, where possible of the solvent molecules is absent [1,2]. It was concluded, in the presence of hydrogen bonding (HB) between the two tautomeric groups, that the intramolecular hydrogen bonding along the corresponding HB is assumed to be the main pathway for many tautomerisations. IHB has been found to govern the conformational preference of molecules [3]. Recent years have witnessed an increase interest in studying the IHB reaction [4-13], theoretically and experimentally. Pauling [14] pointed out that in most cases the strength of the H-bond increases with the increase of the electronegativity value of the acceptor atom. This is exactly the case for oxygen and nitrogen atoms. Particullay, the HBs formed between them and the NH and OH groups are usually strong, which play essential roles in studies in supramolecular, crystal engineering, materials, and life sciences [15].

Last decades have received great efforts to calculate the HB strengths [16-18]. Recently, it was established that the HB strength can be also estimated by looking at the electron density at the bond critical point (BCP) derived from AIM of Bader [19]. This density has been successfully used not only to characterize hydrogen bondings [4-6,12], but also to design new partition schemes as useful tools to investigate the nature of these kinds of weak interactions.

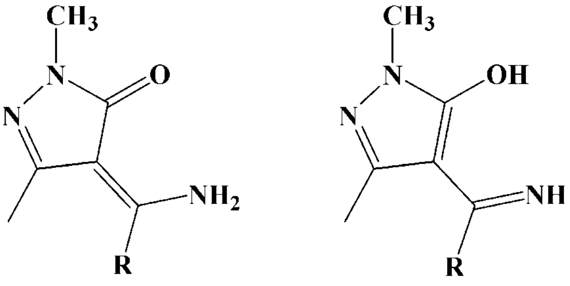

AMP **IMP**

R = H, CH_3, C_6H_5, NH_2, F, Cl and NO_2

Scheme 1

For this study, 4-aminomethylene of 1-methylpyrazolin-5-ones (AMP) and its imine tautomer, IMP, and some of their derivatives (CH_3, F, Cl, C_6H_5, NH_2, and NO_2) have been chosen (see Scheme 1). These compounds are important compounds with widespread use as ligands to obtain metal complexes [20] (as herbicides and fungicides). Furthermore, these compounds have the possibility to undergo the enamine-keto ↔ imine-enol transformation, which is expected to achieve through the IHB the IPT process**.**

The main aim of the current study is to investigate the properties of N-H···O and O-H···N IHBs, which exit for AMP and its IMP tautomer. Therefore, the substitution effect on the hydrogen bond strength and the geometry of the IHB systems were studied. For such investigation, the density functional theory (DFT) and the quantum theory of atoms in molecules of Bader are applied. To obtain more information of the nature of the IHBs; the natural bond orbital analysis (NBO), IR frequencies, and NMR chemical shifts were also considered. Finally the relative strength of the two tautomers and their derivatives were reported.

MATERIALS AND METHODS

COMPUTATIONAL PROCEDURES

All computations were performed at the DFT B3LYP computational level in conjunction with the 6–311+G(d,p) basis sets, using Gaussian09 suite of packages [21]. The geometries of the compounds under probe were fully optimized without the constraint on a possible planarity. For each stationary point, we carried out vibrational frequency calculation at the same level to characterize their nature as local minima or transition states and to find the vibrational N-H and O-H stretching frequencies of the stationary points in the IHB systems under probe. Also, the vibrational calculations were used to correct energies for zero-point energy and thermal contribution. In order to ensure the reliability of the calculated relative stabilities, final energies were obtained through single point calculations, carried out with a 6-311++G(2df,2p) basis set. The reported energy values were rescaled to the single point energy + ZPVE and given in kcal/mol. To obtain more insight into the nature of the IHB system, Bader's QTAIM [19,22,23] was applied. The AIM computations were carried out by using the AIM2000 program [24] to localize bond critical points (BCPs) and ring critical points (RCPs) to characterize them in terms of electron densities (ρ_{BCP}'s and ρ_{RCP}'s) and their Laplacians ($\nabla^2\rho_{BCP}$'s and $\nabla^2\rho_{RCP}$'s). The total electron energy density at the H···O and H···N critical points (HO and HN) is also given for intramolecular HBs. For the latter value its components are considered: the potential electron energy density (V_{BCP}) and the kinetic electron energy density (G_{BCP}). For a better understanding of the intramolecular interactions, the natural bond orbital (NBO) [25] analysis were carried out. Finally, correlations between some calculated parameters with IHB energies, E_{HB} have also been considered. Graphs were drawn and regression analyses were performed using Origin Pro 7.0 software.

RESULTS AND DISCUSSION

AIM analysis of intramolecular H-bonds

Bader's QTAIM [19] provides a solid foundation for the estimation of the strength of IHB [26-30]. This theory is based on topological properties of the electron density (ρ), and Laplacian of the electron density ($\nabla^2\rho$) at the bond critical points (BCP) of two hydrogen bonded atoms. Therefore, the analysis of bond critical points was applied in order to obtain the IHB energy, E_{HB}. It was pointed out that there is a well known relation Eq. (1) between Laplacian and the energetic characteristics of the critical point

$$\frac{1}{4}\nabla^2\rho_{BCP} = 2G_{BCP} + V_{BCP} \qquad \text{and} \quad H_{BCP} = G_{BCP} + V_{BCP} \qquad (1)$$

where G_{BCP} and V_{BCP} are, respectively, the kinetic and potential electron energy densities at BCP. It is worthy to mention that knowing of the BCP in the hydrogen bond and the ring critical point (RCP) in the quasi ring associated to the formation of the IHB between the two bonded atoms is very useful to characterize the IHB. Several theoretical methods [17,31] have been proposed to estimate hydrogen bond energy. One of the most useful of these methods has been explained by Espinosa et al [32] who found that IHB energy, E_{HB}, may be correlated with the potential electron energy density at BCP by the expression $E_{HB} = V(\rho_{BCP})/2$. Grabowski [29] pointed out that the H-bond energy is related to (ρ) at the H···Y (O or N) BCP and ($\nabla^2\rho$), of electron density at BCP of two hydrogen bonded atoms. If a H-bond exists, then the range of ρ_{BCP} and $\nabla^2\rho_{BCP}$ are 0.002–0.035 and 0.024–0.139 a.u., respectively.

Table 1 displays the calculated total electronic density, ρ, and its corresponding Laplacian, $\nabla^2(\rho)$ at BCP and RCP, potential electron energy density, V_{BCP}, kinetic electron energy density, G_{BCP}, ratio of |*G(r)/V(r)*| at BCP, and IHB energy for AMP and IMP tautomers and their derivatives. An inspection of Table 1 indicates that the H···O and H···N contacts have the following topological properties as follows:

- H···N and H···O contacts had low ρ_{BCP} and the that of the former is lower than that of the latter,
- Both bridges had positive $\nabla^2\rho$ values,
- H···N bonding had positive values and H···O had negative values,
- |*G(r)/V(r)*| values are greater than unity in IMP and less than unity in AMP, reflecting that IHB is of non-covalent nature (electrostatic) in the former and of covalent nature in the latter.
- The electron density and its Laplacian at the RCP, ρ_{RCP} and $\nabla\rho_{RCP}$ of the quasi rings, which are created due to the formation of the IHBs had positive values.
- The properties ρ_{RCP} and $\nabla\rho_{RCP}$ are larger in IMP than in AMP ones.

These properties are typical for closed-shell interactions as IHBs and indicate electrostatic character of the H···O and H···N bondings. Additionally, the calculated Laplacians (not shown) at BCP for N-H bond in AMP and O-H bond in IMP had negative values, thus pointing out that both bonds in both formers have covalent character. In general, the strength and the length of the chemical bond are closely correlated. The bond strength is determined by accumulation of electron density in the bond region and the screening of nuclei by this density [30]. These characteristics of electron densities and its Laplacian at BCPs signify the presence of H-bond interaction. According to Table 1, comparison between the topological parameters of AMP and IMP forms and their derivatives led us to conclude that the IHBs in IMP form are stronger than in AMP forms.

Rozas et al [33] explained that hydrogen bonds can be classified as follows:

- Weak hydrogen bonds (E_{HB} < 12.0 kcal/mol): $\nabla^2\rho_{BCP} > 0$ and $G_{BCP} + V_{BCP} > 0$;
- Medium hydrogen bonds (12.0 < E_{HB} < 24.0 kcal/mol): $\nabla^2\rho_{BCP} > 0$ and $G_{BCP} + V_{BCP} < 0$;
- Strong hydrogen bonds (E_{HB} > 24.0 kcal/mol): $\nabla^2\rho_{BCP} < 0$ and G_{BCP} + VBCP <0;

Table 1 Topological parameters (in a.u) and IHB energies, E_{HB}, (kcal/mol) for AMP (upper) and IMP (lower) and their derivatives calculated on the B3LYP/6-311+G(d,p) wavefunctions.

R	ρ_{BCP}	$\nabla^2\rho_{BCP}$	G_{BCP}	V_{BCP}	$G_{BCP}+V_{BCP}$	$\lvert V_{BCP}/G_{BCP}$	ρ_{RCP}	$\nabla^2\rho_{RCP}$	E_{HB}
	Data for H···O IHB exist in AMP tautomer								
NO_2	0.0278	0.0988	0.0228	-0.0209	0.0019	0.9167	0.0147	0.0914	-6.6
Cl	0.0293	0.1004	0.0236	-0.0222	0.0014	0.9407	0.0150	0.0942	-7.0
F	0.0276	0.0942	0.0219	-0.0203	0.0016	0.9269	0.0145	0.0908	-6.4
H	**0.0240**	**0.0850**	**0.0192**	**-0.0172**	**0.0020**	**0.8958**	**0.0135**	**0.0828**	**-5.4**
CH_3	0.0288	0.1008	0.0236	-0.0219	0.0017	0.9280	0.0150	0.0939	-6.9
C_6H_5	0.0294	0.1026	0.0241	-0.0226	0.0015	0.9378	0.0151	0.0947	-7.1
NH_2	0.0318	0.1067	0.0257	-0.0248	0.0009	0.9650	0.0157	0.0987	-7.8
	Data for H···N IHB exist in IMP tautomer								
NO_2	0.0380	0.0985	0.0278	-0.0309	-0.0031	1.1133	0.0171	0.1019	-9.7
Cl	0.0365	0.0946	0.0263	-0.0289	-0.0026	1.0992	0.0167	0.0992	-9.1
F	0.0343	0.0914	0.0246	-0.0263	-0.0017	1.0698	0.0163	0.0956	-8.2
H	**0.0431**	**0.0988**	**0.0305**	**-0.0363**	**-0.0058**	**1.1906**	**0.0174**	**0.1070**	**-11.4**
CH_3	0.0488	0.1017	0.0343	-0.0430	-0.0087	1.2531	0.0184	0.1133	-13.6
C_6H_5	0.0507	0.1027	0.0357	-0.0456	-0.0099	1.2773	0.0186	0.1152	-14.3
NH_2	0.0518	0.1022	0.0362	-0.0469	-0.01069425	1.2954	0.0187	0.1159	-14.7

According to our theoretical results in Table 1 and the above classification of the IHB, it can be concluded that the O-H···N IHB exist for IMP is of medium power hydrogen bond, while the O-H···N IHB exist for AMP is weak hydrogen bond. It was shown that topological parameters at BCP and RCP may be useful to describe the strength of IHB [7,34,35]. The correlation of IHB energies, E_{HB}, of the N-H···O and the O-H···N bridges with the $|V_{BCP}/G_{BCP}|$ ratio, total electronic density and its corresponding Laplacian in BCPs are shown in Figure 1. The linear dependence with high regression coefficients (close to unity) indicates that there is strong correlation between IHB energies and the abovementioned topological properties. These findings illustrate that these quantum descriptors can be used to estimate the hydrogen bond strength.

The existence of the ring critical point (RCP) in the chelated ring structure, which is created due to the formation of the IHB, was analyzed. Grabowski [29] pointed that for IHBs there is a correlation between the hydrogen bond strength, E_{HB}, with the total electron density, ρ, and its Laplacian, ∇^2_ρ at RCP. For the systems under probe there are a good linear correlations between E_{HB} and the topological properties at the RCP, ρ_{RCP} and ∇^2_ρ, with a correlation coefficients are very high (near to one) as can be shown in Figure 2 (a-d). Our findings indicate that the topological properties at the ring critical point can also be used to estimate the relative strength of the IHB. Comparison of the topological properties calculated at RCP and BCP indicates that the OH···N IHBs exist for IMP forms are stronger than the NH···O IHBs exist for AMP forms.

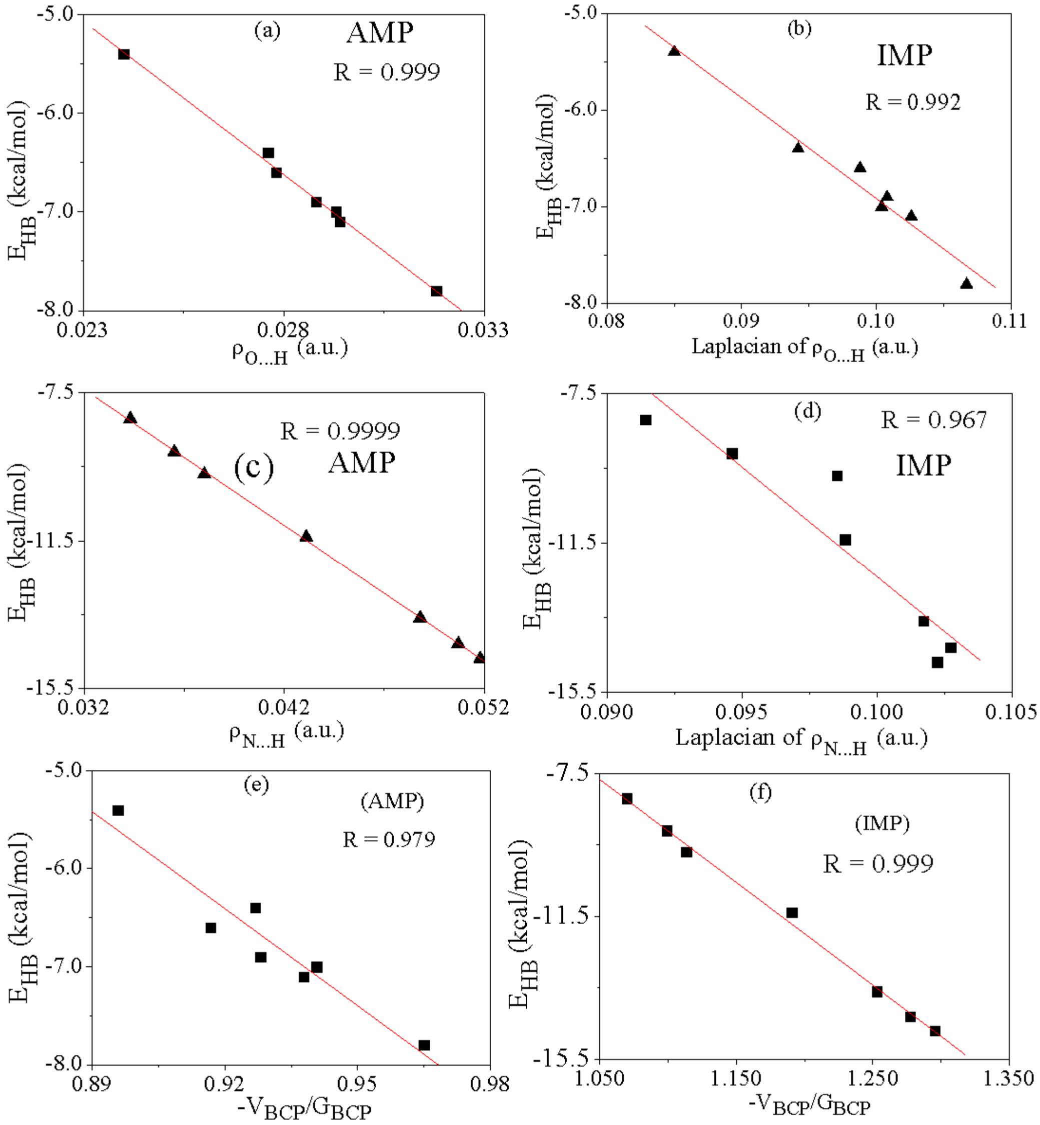

Figure 1: *Left:* E_{HB} of O···H IHB in AMP vs. (a) Total electronic density at O···H BCP (c) Laplacian of total electronic density at O···H BCP and (e) $|V_{BCP}/G_{BCP}|$ ratio at O···H BCP. *Right:* E_{HB} of N···H IHB in AMP vs. (a) Total electronic density at N···H BCP (c) Laplacian of total electronic density at N···H BCP and (e) $|V_{BCP}/G_{BCP}|$ ratio at N···H BCP.

On the other hand, Table 1 shows variation of the E_{HB}, ρ_{BCP}, and $\nabla^{2}{}_{\rho}$ properties at both BCP and RCP depend on the nature of the substituent groups. Substitution of the electron-withdrawing groups (F, Cl and NO_2) tends to reduce these parameters and weakness the hydrogen bond. The reverse action is true in the case of electron donating groups (CH_3, C_6H_5 and NH_2). For example, the strongest hydrogen bond was reported for NH_2 group and the weakest one was found for F group.

Geometrical analysis of intramolecular H-bonds

The most relevant geometrical structural parameters, associated with the formation of NH···O and OH···N IHBs exists for AMP and IMP tautomers, respectively, are summarized in Table 1. The optimized structures of the parent tautomers AMP-H and IMP-H are shown in Figure 3. The optimized structures of all derivatives of AMP and IMP tautomers and the transition states which connect them are available from the author upon request.

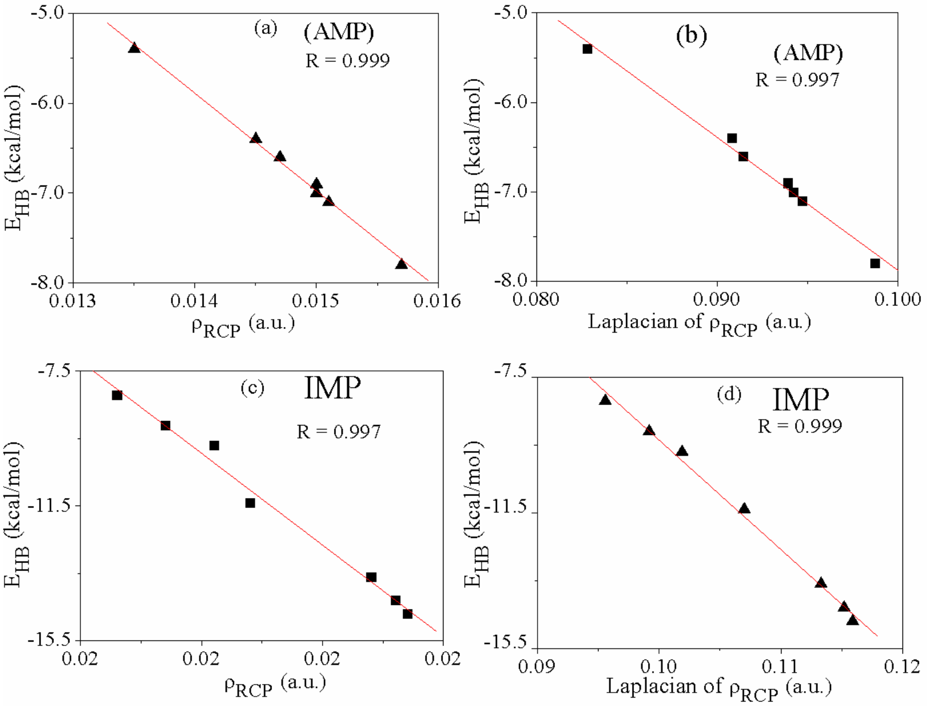

Figure 2: ***Left:*** **E_{HB} of O···H IHB in AMP vs. (a) Total electronic density at O···H BCP and (c) Laplacian of total electronic density at O···H BCP.** ***Right:*** **E_{HB} of N···H IHB in AMP vs. (b) Total electronic density at N···H BCP and (d) Laplacian of total electronic density at N···H BCP.**

According to Table 2, for AMP forms, despite of the nature of the substituent, the N-H bond becomes longer and N···O and the NH···O IHB distances become shorter than those in the parent tautomer (AMP-H). For IMP forms, the picture is completely different, it is found that on going from an electron withdrawing substituent group to an electron donating one, OH···N IHB and O···N distances become shorter and the O-H bond becomes longer when compared with those of the parent molecule (IMP-H). As it is obvious from Table 2, the geometrical properties of AMP and IMP forms illustrate that the ranges of O···N and H···N distances in IMP tautomer are about 0.013-0.119 Å and 0.058-0.188 Å shorter than those in AMP ones. Additionally, the valence angle θ_{OHN} in IMP forms is about 7.4–12.6° higher than in the AMP ones. These facts predict that the OH···N IHB is stronger than the NH···O one. As shown in Figure 4 (a-d), IHB energies of the H···O and H···N bridges, E_{HB}, correlate well with the geometrical parameters (O-H covalent bond, H···O and H···N hydrogen bonds, O···N contacts and N-H···O and O-H···N bond angles). The linear correlation coefficients are 0.998, 0.999, 0.996, 0.926, 0.870, 0.991, 0.951 and 0.994, respectively.

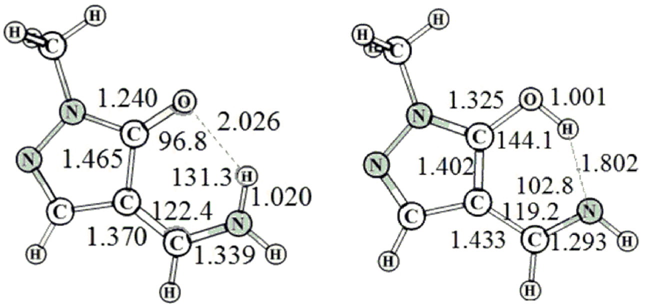

AMP-H IMP-H

Figure 3: Geometrical structure of the parent AMP and IMP tautomers.

Table 2. Selected geometrical parameters (distances in Å and angles in ◦) for AMP (upper) and IMP (lower) and their derivatives calculated at B3LYP/6-311+G(d,p) level of theory.

R	AMP				IMP			
	□□H	H···O	N·····O	$\square_{\square\square\square\ldots\square}$	□–□	H···□	N·····O	$\square_{\square\square\square\ldots\square}$
NO_2	1.021	1.949	2.739	132.0	0.992	1.85	2.702	142.1
Cl	1.026	1.925	2.745	134.6	0.992	1.871	2.723	142.0
F	1.025	1.955	2.759	133.1	0.991	1.897	2.746	141.8
H	**1.02**	**2.016**	**2.806**	131.5	**1.001**	**1.802**	**2.678**	144.1
CH_3	1.023	1.932	2.749	134.6	1.007	1.751	2.64	144.9
C_6H_5	1.023	1.923	2.747	135.5	1.009	1.735	2.627	145.1
NH_2	1.027	1.888	2.741	138.3	1.012	1.724	2.622	145.7

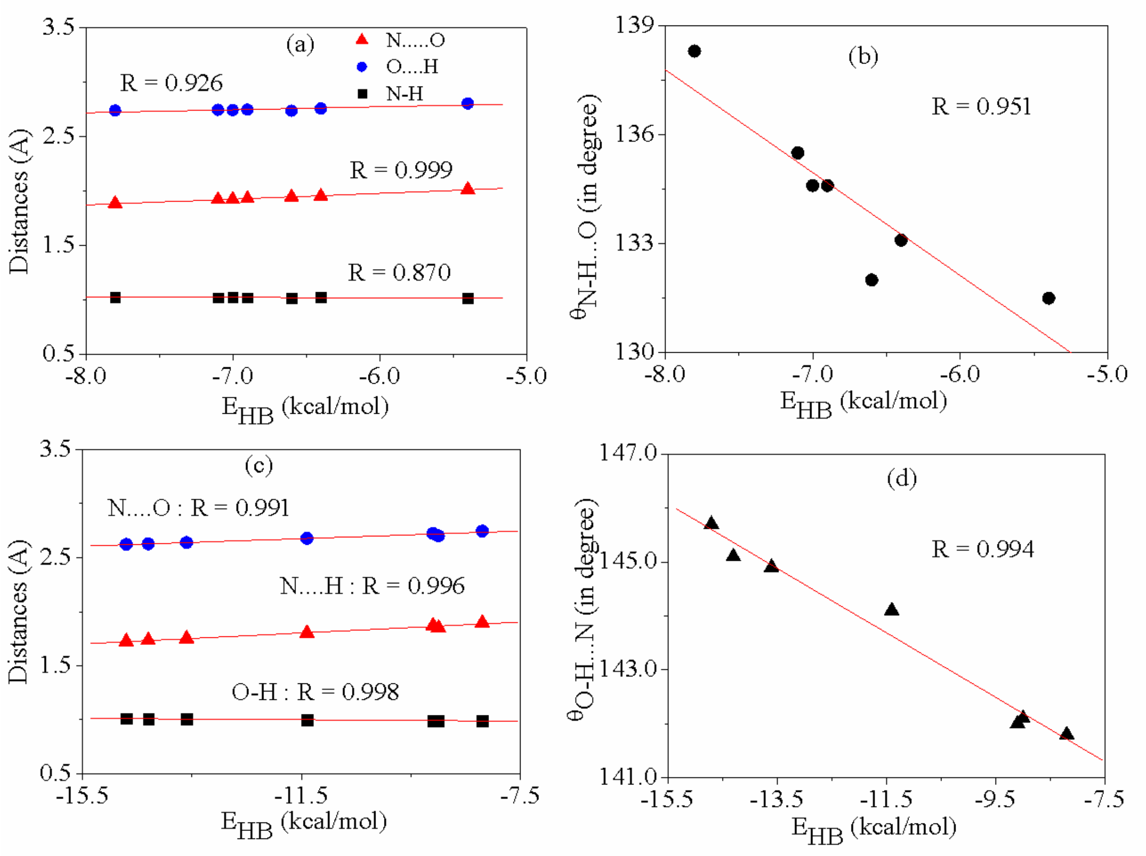

Figure 4: Linear correlation dependencies of (a) E_{HB}(H···O) vs. N-H, H···O and N····O distances (AMP), (b) E_{HB}(H···O) vs. $\theta_{N\text{-}H\cdots O}$ (AMP) (c) E_{HB}(H···N) vs. N-H, H···N and N····O distances (IMP) and (d) E_{HB}(H···N) vs. $\theta_{O\text{-}H\cdots N}$ (IMP)

As can be shown in Figure 5 (a and b) of the supplementary information, the correlation of E_{HB}(H···O) with the sum of N-H bond length and H···O distance (R = 0.988) is considerably better than the correlation between E_{HB}(H···O) and O···N distance (R = 0.870), which is not as good as with the other geometrical parameters. On the other hand, correlation of E_{HB}(H···N) with the sum of O-H bond length and H···N distance (R = 0.999) is considerably as good as the correlation of E_{HB}(H···N) with H···N distance (R = 0.991). Previous studies [36] attributed this behavior to the non-linearity of the hydrogen bond system. Also, Table 2 shows, in general, for IMP forms, electron donating groups (CH_3, C_6H_5 and NH_2) lengthen the N-H covalent bond and shorten H···N and O···N distances in comparison with the parent molecule. The opposite effect is true in case of electron with drawing substituent groups (NO_2, F and Cl). For AMP, the picture is more complicated (as can be shown in Table 2). It is worthy to mention that, there are some invaluable correlations between topological and geometrical parameters (not shown). For example, a good correlation between H···N and $\rho_{H\cdots N}$ exists with R value amount to 0.998 (with equation as $\rho_{H\cdots N}$ = - 0.103 $d_{H\cdots N}$ + 0.229) for IMP form. Again, similar correlation between H···O and $\rho_{H\cdots O}$ exists with R value amounts to 0.856 (with equation as $\rho_{H\cdots N}$ = - 8.409 $d_{H\cdots O}$ + 2. 993) for AMP form. All these results illustrate that the topological properties and the geometrical parameters can be used as a good descriptor to estimate the hydrogen bond.

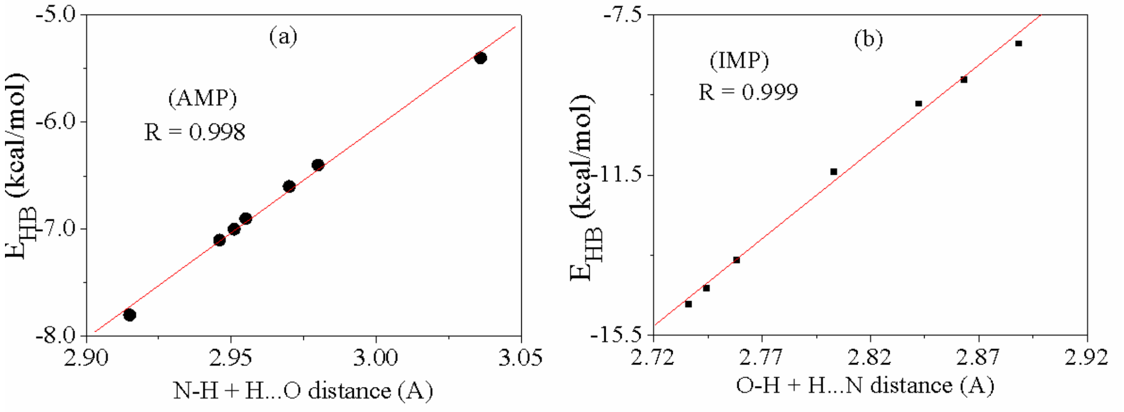

Figure 5: (a) E_{HB} of O···H IHB in AMP vs. N-H+H···O distances. (b) E_{HB} of N···H IHB in IMP vs. O-H+H···N distances.

NBO analysis

In the NBO analysis, the electronic wave functions are interpreted in terms of a set of occupied Lewis and a set of non-Lewis localized orbitals [37]. Delocalization effects can be identified from the presence of off diagonal elements of the Fock matrix. The strengths of these delocalization interactions, E_{CT}, are estimated by second order perturbations theory. It is well known that in the NBO analysis of H-bond systems, the charge transfer between the lone pairs of proton acceptor and antibonds of proton donor is highly important.

The results of NBO analysis clarify that in the quasi ring structure of AMP and IMP tautomers, the lone pair of nitrogen atom (LP(N)) and the two lone pairs of oxygen atom, LP(O), respectively, participate as donors and the σ^*_{O-H} and σ^*_{N-H}, respectively, interactions behave as acceptors in strong intramolecular charge transfer interaction and their energies are presented in Table 3.

Table 3: Frequency of ν_{N-H} and ν_{O-H} stretching vibrational modes, frequency shifts (Δν = Δν(R) - Δν(H), and charge transfer energy, E_{CT}, (kcal/mol) for, respectively, AMP and IMP tautomers and their derivatives calculated at B3LYP/6-311+G(d,p) level of theory.

R	AMP				IMP			
	ν_{N-H}	$\Delta\nu_{N-H}$	δ^1H	$E_{CT}^{(a)}$	ν_{O-H}	$\Delta\nu_{O-H}$	δ^1H	$E_{CT}^{(b)}$
NO_2	3401	32	9.3	8.3	3292	171	11	18.3
Cl	3327	105	9.8	9.7	3297	176	10.6	14.8
F	3354	79	9.2	8.7	3325	204	10.3	13.9
H	**3432**	**0**	**9.1**	**6.2**	**3121**	**0**	**12.3**	**20.9**
CH_3	3379	53	10	9.1	3019	103	13	25.3
C_6H_5	3370	63	10.2	9.4	2985	136	13.5	-
NH_2	3313	120	9.9	11.2	2952	169	13.3	28.5

(a)Corresponds to LP(O) →σ^*_{N-H} antibonding interactions; (b)Corresponds to LP(N) →σ^*_{O-H} antibonding interactions.

As it is common, the orbital energies, E_{CT}, have been reported in kcal/mol. These energies correspond to the LP(N) → σ^*_{O-H} and LP(O) → σ^*_{N-H} interactions, respectively, which is related to maximum LP(N) → σ^*_{O-H} and LP(O) → σ^*_{N-H} overlaps leading to a linear or close to linear geometry in the O-H···N and N-H···O hydrogen boning systems, respectively. In the current research, the H-bond leads to an increase in the σ^*_{O-H} and σ^*_{N-H} antibonding orbital occupancy, producing the weaker and longer O-H and N-H bonds. Close look at the tabulated results in Table 3 indicate that the nature of the substituent influences the strength of the N-H···O and O-H···N intramolecular hydrogen bondings according to the following trends AMP-NH_2 > AMP -C_6H_5 > AMP -CH_3 > AMP -Cl > AMP -F > AMP -NO_2 > AMP -H and IMP -NH_2 > IMP -CH_3 > IMP-H > IMP-F > IMP-Cl > IMP-NO_2, respectively.

It is important to mention that that NBO energy, E_{CT}, related to LP(NO) → σ^*_{O-H} and LP(O) → σ^*_{N-H}, overlaps nicely correlates with other geometrical and topological parameters. For example, the linear correlation coefficients showing E_{CT} dependency versus H···O and H···N contacts are 0.981 and 0.990, respectively (not shown). Also, the linear correlation coefficients showing the dependency of E_{CT} versus $\rho_{H\cdots O}$ and $\rho_{H\cdots N}$ are 0.996 and 0.995, respectively (not shown). Furthermore, there is a decent linear relationship between E_{HB} with $E_{CT,}$ with the correlation coefficients amount to 0.991 and 0.996, respectively. These results provide that the properties of the charge transfer between the lone pairs of proton acceptor and antibonds of proton donor (E_{CT}) could be very useful in estimating the IHB strength.

IR and NMR:

Anotherr approach used to study the strength of the hydrogen bondings in the investigated species is the IR spectroscopy of the O-H and N-H bonds on the one hand and the ^{1}H NMR chemical shifts (δ^1H) of the donor hydrogen atom involved in IPT process. It is well known that there is a good correlation between frequency shift of the stretching vibration mode, *ν*, of the accepted bond and the IHB strength. Espinosa et al[32] used such this correlation for the estimation of the IHB strength.

The calculated frequency shifts of N–H, $\Delta\nu_{N-H}$, and O-H, $\Delta\nu_{O-H}$, stretching vibration modes for parent tautomers (respectively, AMP and IMP) and their derivatives are tabulated in Table 3. The frequency shifts with respect to the parent AMP and IMP tautomers, Δν, are plotted against IHB energies, E_{HB}, in Figure 6 (c) and (d), respectively. In substituted tautomer AMP, regardless of the nature of substituent, *ν*(N–H) mode shows a negative frequency shift (red shift). In substituted tautomer IMP, *ν*(O–H) mode shows a negative frequency shift (red shift) in case of electron donating substituent groups and a positive frequency shift (blue shift) in case of electron withdrawing substituent ones. The highest red shift is observed for NH_2 substituent which is in agreement with the highest E_{HB} and the lowest red shift is observed for CH_3 susbtituents. On the other hand, the highest blue shift is observed for fluorine substituent and the lowest one is reported for nitro group which is also in agreement with the H-bond energy (see Table 3). As presented in Figure 6 (a and b), the H-bond energies, E_{HB}(N···H) and E_{HB}(O···H), correlate well *Δν*(O–H) and *Δν*(N–H) for IMP and AMP tautomers. The larger negative shift shows higher E_{HB} and larger positive shift shows lower E_{HB}.

Another sensitive descriptor to measure the E_{HB} is the ^{1}H NMR chemical shift (*δ*) of the hydrogen atom which involved in the IHB [38]. Formation of the intramolecular H-bonds leads, as a rule, to deshielding of bridged hydrogen atom and consequently to an increase in its chemical shift. ^{1}H NMR chemical shifts , δ^1H, of the parent tautomers (AMP and IMP) and their derivatives are tabulated in Table 3. The ^{1}H NMR values were calculated by means of gauge-independent atomic orbital (GIAO) method [39] at the B3LYP/6-311+G(d,p) level of theory. The calculated chemical shielding were converted into chemical shifts (δ) by subtracting 31.76, the ^{1}H shielding of tetramethylsilane computed at the same level of theory and basis set. It was pointed that the stronger IHB causes the δ^1H chemical shift of donor atom, H, to move downfield further. From Table 3 it is obvious that the calculated δ^1H values for AMP species, regardless of the substituent group, are upfiled and those in the case IMP species are downfield. The main effect of the electron donating substituent groups (in contrary of the electron withdrawing substituent groups) is increasing of δ^1H chemical shifts of the donor H atom. According to the above observations, it is clear that the IHB in IMP species (O-H···N) are stronger than those in AMP forms (N-H···O).

Figure 4 (e and f) presents the graphical plotting of δ^1H versus H-bond energy, E_{HB}, of the AMP and IMP, respectively. The linear correlation coefficients of these dependencies are very high in case of IMP tautomer (R = 0.994) and it is not good in case of AMP species (R = 0.881). Moreover, our results indicates that there is a good correlation between δ^1H NMR chemical shifts and E_{CT}, related to LP(N) → σ^*_{O-H} and LP(O) → σ^*_{N-H} interactions. The correlation coefficients of the aforementioned dependencies are 0.971 and 0.635, respectively. These kinds of dependencies are important, because they allow us to estimate quantitatively the strength of such interactions and provide a physical explanation for the process.

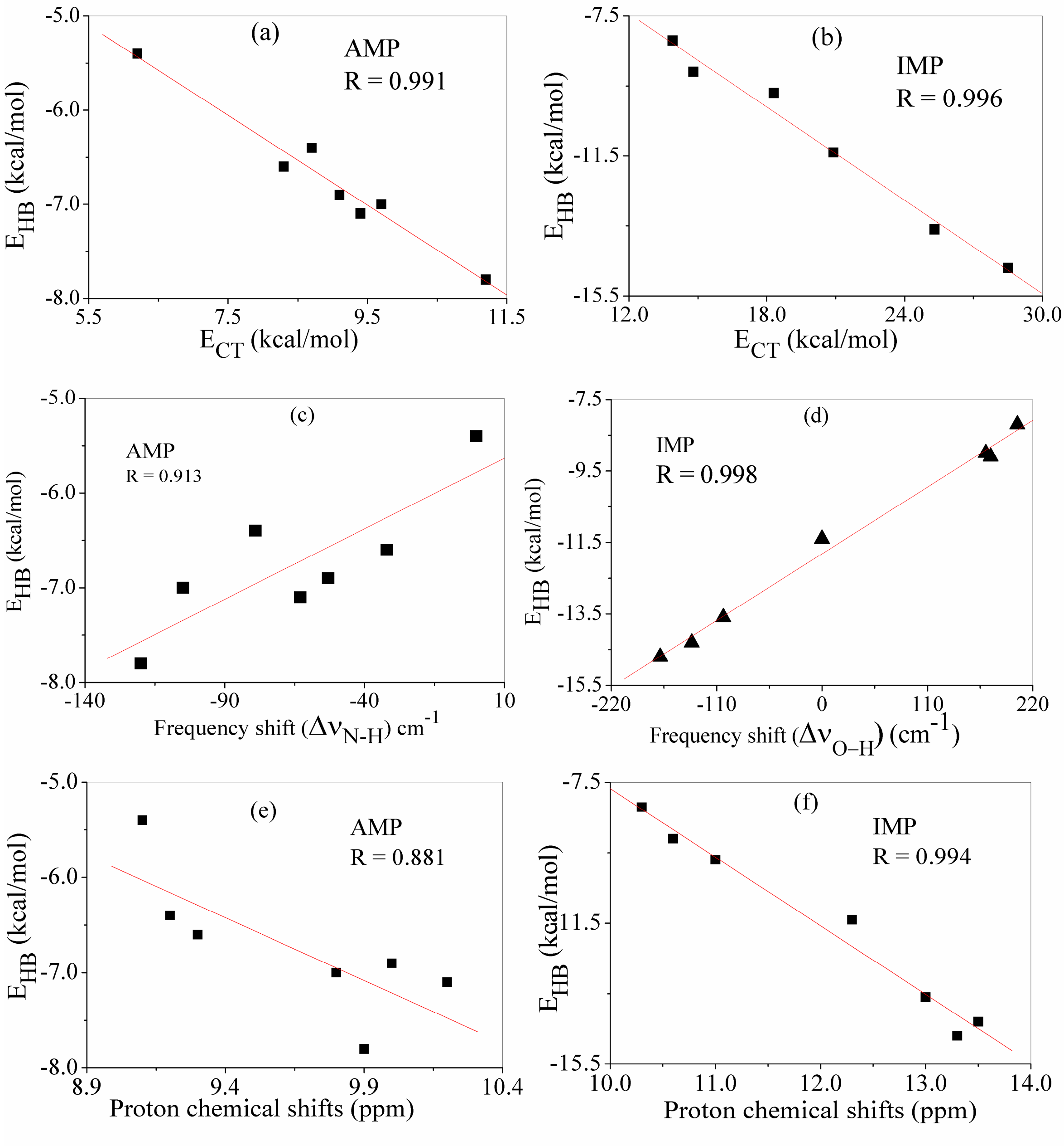

Figure 6: ***Left:*** **E_{HB}(O···H in AMP) vs. (a) Frequency shifts, $\Delta\nu_{N\text{-}H}$ (c) E_{CT}, related to LP(O)→$\sigma^*_{N\text{-}H}$ and (e) proton chemical shifts δ^1H.**
Right: Left: **E_{HB}(O···H in AMP) vs. (b) Frequency shifts, $\Delta\nu_{O\text{-}H}$ (d) E_{CT}, related to LP(N)→$\sigma^*_{O\text{-}H}$ and (f) proton chemical shifts δ^1H.**

Table 4: Relative energies, □E=(AMP-IMP) and the relative energy gap between E tautomer and the transition state, □E=(AMP-TS). All values are in kcal/mol.

	ΔE(AMP-IMP)	ΔE(AMP-TS)
$-NO_2$	4.1	2.7
-Cl	3.0	1.5
-F	2.1	1.2
-H	7.5	4.5
$-CH_3$	7.6	4.0
$-C_6H_5$	7.6	3.9
$-NH_2$	5.5	1.7

Analysis of Tautomers Stabilities

The relative energies of the AMP and IMP tautomers (Scheme 1) are tabulated in Table 4. The total set of data is summarized in Table 5 of the Supplementary Materials. Comparison of the relative energies of AMP and IMP tautomers, $\Delta E = E_{AMP}\text{-}E_{IMP}$, shows, regardless of the nature of the substituent, that AMP tautomers are more stable than IMP ones, which is in agreement with the previous experimental results [20,40]. As it is obvious from Table 1 that the relative stability difference is significant and it is ranged from 2.1-7.6 kcal/mol.

Close look At table 1 illustrates that the nature of the substituent influences the energy gap between the tautomers in favor of AMP form, the greater the electron donating effect of the substituent (NH_2, CH_3, C_6H_5), the more energy difference. According to these results it can be concluded that AMP tautomer is the predominat one in gas phase. Furthermore, the energy gap which connects the most stable tautomer and the transition state, (ΔE(AMP-TS)) is considerably small (ranging from 1.2 to 4.5 kcal/mol). This implies that the IMPT reaction, if proceed, is thermodynamically possible and the considered tautomers (AMP and IMP) may interchangeable. According to Table 4, one can conclude that the highest degree of equilibrium between the AMP and IMP tautomers is observed for R = -F, with ΔE = 1.2 kcal/mol, whereas the least one is reported for R = -H, with ΔE= 4.5.

Table 5: Optomized energies, Eopt, Single point energies, E_{sp}, zero point energies, ZPE, and Thermal correction to energy, TCE (All values are in hartree).

	E_{opt}	E_{sp}	ZPE	TCE
AMP-H	-434.336157	-434.362794	0.125352	0.13383
IMP-H	-434.324147	-434.350857	0.125512	0.13368
TS	-434.32033	-434.347115	0.121501	0.12914
AMP-CH3	-473.668471	-473.697715	0.152533	0.16283
IMP -CH3	-473.656992	-473.686133	0.153066	0.16282
TS	-473.653945	-473.683213	0.148868	0.15829
AMP-F	-533.607910	-533.639776	0.116928	0.12631
IMP-F	-533.606034	-533.637747	0.117766	0.12673
TS	-533.598021	-533.630005	0.113396	0.12187
AMP-Cl	-893.95826	-893.989326	0.115370	0.12505
IMP-Cl	-893.955149	-893.985812	0.116134	0.12548
TS	-893.947944	-893.978945	0.111788	0.12062
AMP- NH2	-489.723482	-489.753749	0.14227	0.15203
IMP-NH2	-489.714315	-489.744639	0.142162	0.15171
TS	-489.711574	-489.742047	0.137989	0.14723
AMP-C6H5	-665.449854	-665.491599	0.206239	0.21912
IMP-C6H5	-665.437588	-665.479343	0.206265	0.21891
TS	-665.435072	-665.476998	0.20232	0.21455
AMP-NO2	-638.890353	-638.929761	0.127094	0.13801
IMP-NO2	-638.884965	-638.924221	0.127698	0.13844
TS	-638.877808	-638.917354	0.123325	0.13355

CONCLUSION

We have investigated the intramolecular hydrogen bondings exit in AMP and IMP tautomers and their derivatives using B3LYP level of theory at the 6-311+G(d,p) basis set. The energetic results obtained from DFT calculations suggest, in all cases, that the AMP tautomer is more stable than IMP one. The results obtained from the geometrical and topological parameters derived from Bader's theory suggest that the stronger IHB can lead to lengthening N-H and O-H bonds and shortening the intramolecular hydrogen bondings (H···O and H···N) and the N···O distances. Our calculated RCPs values are useful descriptor of the strength of intramolecular H-bonds. There is a decent correlation exists between IHB energy, E_{HB}, and the structural, topological parameters, 1H NMR and charge transfer energy, E_{CT}, derived from NBO calculation. It can be concluded that E_{HB} calculated from the topological parameters may be treated as the HB energy, and well correlates to the pertinent IHB strength parameters. Moreover, the calculated electron densities and Laplacian properties of AMP and IMP tautomers illustrate that H···O and H···N bondings have lower ρ and positive $\nabla^2{}_\rho$ values, which is typical for closed-shell interaction indicating electrostatic character of the H···O and H···N bondings. The numerous linear relationships with very high correlation coefficients found in this study strongly assume that the aforementioned parameters may be very useful to evaluate the H-bond strengths.

Acknowledgments
A generous allocation of computational time at the Scientific Computational Center (CCC) of the Universidad Autónoma de Madrid (Spain) acknowledged.

REFERENCES

[1] Y Gauduel, PJ Rossky In: *Ultrafast Reaction Dynamics and Solvent Effects*, Part III, AIP Press, New-York, **2006**, p. 173.
[2] T Bountis, *Proton Transfer in Hydrogen-Bonded Systems*, Plenum Press (ed.), NY, **1992**, p. 365.
[3] CJ Duarte; MP Freitas, *J. Mol. Struct.*, **2009,** *930* 135-139.
[4] SJ Grabowski, *J. Phys. Chem. A*, **2000**, *104* 5551-5557.
[5] SJ Grabowski, *J. Mol. Struct.***, 2000,** *553* 156.
[6] SJ Grabowski, *J. Phys. Chem. A*, **2001**, *105* 10739-10746.
[7] S Wojtulewski; SJ Grabowski, *J. Mol. Struct. (Theochem)* **2003**, *621* 285-291.

[8] S.J. Grabowski; M Małecka, *J. Phys. Chem. A,* **2006,** *110* 11847-11854.
[9] H Raissi; M Yoosefian; S Khoshkhou, *J. Comput. Theor. Chem.***,** **2012**, 983 1-6.
[10] M Yoosefian; H. Raissi; ES Nadim; F Farzad; M Fazli; E Karimzade; AR Nowroozi, *Int. J. Quant. Chem.*, **2011,** *111* 3505-3516.
[11] P Sanz; O Mó; M Yanez, J. Elguero, *J. Chem. Phys. Chem.*, **2007,** *8* 1950-1958.
[12] P Sanz; O Mó; M Yanez, J. Elguero, *J. Phys. Chem. A* **2007,** *11*, 3585-3591.
[13] P Sanz; O Mó; M Yanez, J. Elguero, *Chem. Eur. J.* **2008**, *14*, 4225-4232.
[14] L Pauling, *In The Nature of the Chemical Bond*, 3rd ed. Cornell University Press Ithaca New York **1960**.
[15] GA Jeffrey, *An Introduction to Hydrogen Bonding* New York Oxford University Press, **1997**
[16] H Raissi; E Moshfeghi; AF Jalbout; MS Hosseini; M Fazli, *Int. J. Quant. Chem.* **2007,** *107* 1835-1845.
[17] A Nowroozi; H Raissi; F Farzad, *J. Mol. Struct. (Theochem)* **2005,** *730* 161-169.
[18] I Rozas; I Alkorta; J Elguero, *J. Phys. Chem. A* **2001**, *105* 10462-10467.
[19] RFW Bader, *In Atoms in Molecules: A Quantum Theory;* Oxford University press: Oxford, **1990**.
[20] J Belmar; FR Pérez; J Alderete, C Zuniga, *J. Braz. Chem. Soc.* **2005,** *16* 179-189.
[21] MJ Frisch *et al.*, Gaussian 09 Revision-A.02 SMP, Gaussian Inc., Wallingford CT, **2009**.
[22] RFW Bader, *Chem. Rev.* **1991**, *91* 893-928.
[23] RFW Bader, *J. Phys. Chem. A* **1998,** *102* 7314-7323.
[24] F Biegler-Kōnig, AIM2000, University of Applied Sciences, Bielefeld, Germany, **2000**.
[25] ED Glendening; AE Reed; JE Carpenter; F Weinhold, NBO, Version 3.1, Gaussian09 package of programs, Inc., Pittsburgh, PA, **1992**.
[26] MT Carroll, RFW Bader, *Mol. Phys.* **1988**, *65* 695-722.
[27] U. Koch, P. Popelier, *J. Chem. Phys.* **1995**, *99* 9747- 9754.
[28] O Mó; M Yaňez; J Elguero, *J. Mol. Struct. (THEOCHEM)* **1994**, 314 73-81.
[29] SJ Grabowski, *J. Mol. Struct.* **2001**, *562* 137-143.
[30] RFW Bader, *ACC. Chem. Res.* **1985** *18* 9-15.
[31] P Schuster; G Zundel; C Sandorfy, **1976** *The hydrogen bond* (Amsterdam: North Holland Publ. Co.
[32] E Espinosa; E Molins, C Lecomte, *Chem. Phys. Lett.* **1998**, 285 170-173.
[33] I Rozas; I Alkorta, J Elguero, *J. Am. Chem. Soc.***2000,** 122 11154-11161.
[34] D Quiñonero; A Frontera; P Ballester; C Garau; A Costa; PM Deyá, *Chem. Phys. Lett.* **2001,** 39 369-374.
[35] SJ Grabowski, *Monatsch. Chem.***2002**, 133 1373-1380.
[36] S Emamian; SF Tayyari, *J. Chem. Sci.***2013**, 125 939–948.
[37] AE Reed; LA Curtis; FA Weinhold, *Chem. Rev.* **1988,** *88* 899-926.
[38] N Trendafilova; G Bauer; T Mihaylov, *Chem.Phys.* **2004,** 302 95-104
[39] K Wolinski; JF Hinton; P Pulay, *J. Am. Chem. Soc.* **1990,** *112* 8251-8260.
[40] ZS Safi; HM Alhendawi, *Asian J. Chem.* **2009**, **21** 4772-4784.